22nd Australasian Fluid Mechanics Conference AFMC2020
Brisbane, Australia, 7-10 December 2020
https://doi.org/10.14264/99dec0a

Numerical Study of the Flow Behaviour of Discocyte Red Blood Cell Through a Non-uniform Capillary

D.M.W. Karandeniya[1], D. Holmes[1], E. Sauret[1] and Y.T. Gu[1]

[1]School of Mechanical Medical & Process Engineering

Queensland University of Technology, Brisbane QLD 4000, Australia

Abstract

Red blood cells (RBCs) are the main component of the blood and comprise about 45% of the total volume of blood. The key role of RBCs is to transfer oxygen from pulmonary capillaries to tissue capillaries, and transfer carbon dioxide from tissues to lungs. While some of these capillaries have uniform cross-sections, some non-uniform capillaries are also present. Often the diameters of these cross sections are smaller than the diameter of the RBCs. Yet because of the high deformability of its viscoelastic membrane, the RBCs are able to flow through these capillaries. The purpose of this analysis is therefore to investigate the flow activity of RBCs during their passage through a non-uniform capillary using the Lattice Boltzmann – Immersed Boundary (LB-IB) method.

Keywords

Discocyte, RBCs, Capillaries, LB-IB method

Introduction

Red Blood Cells (RBCs) are the major component in blood and account for approximately 45% of the total blood volume [2]. Healthy RBCs exhibit a discocyte shape with an average diameter of 7.8 μm and 2 μm in average thickness [2, 3]. The average volume of 90 μm^3 and the surface area is about 136 μm^2 [2]. The RBC membrane consists of two main components: a lipid bilayer, in which proteins are embedded, and a 2D cytoskeleton network anchored beneath it [4, 5]. Several skeletal proteins and anionic phospholipids directly interact. This interaction contributes as an additional attachment between the skeletal network and the lipid bilayer [6]. The membrane is highly elastic and rapidly responds to applied fluid stresses.

RBC deformability plays an essential part in providing oxygen to tissues [7]. This is determined by the cell geometry (the large surface area-to-volume ratio of the biconcave disc), the viscoelastic properties of the cell membrane, and the viscosity of the cytoplasmic and extracellular fluids [4]. This research examines the deformation behaviour of discocyte shaped RBCs when flowing through a non-uniform capillary by using Lattice Boltzmann-Immersed Boundary (LB-IB) method to validate the accuracy and efficiency of LB-IB method in advanced numerical modelling for blood flows.

Methodology

The software package HemoCell, a blood - focused framework for simulating dense deformable cell suspensions, is chosen in this study. HemoCell is based on the combined LB-IB method and is built on top of Palabos. Following findings from the literature, LB-IB method was selected as the most efficient method for the modelling [1, 8].

In Hemocell, blood plasma is represented as LB particles, while RBC is represented as discrete element method (DEM) membranes coupled to the plasma flow by IB method [1]. The initial membrane of RBC in Hemocell was characterised by 642 vertices, 1,920 edges with 1,280 resulting faces. This distinct membrane structure can describe the mechanical behaviour of the RBC. The cell's response to deformations is formulated as a series of forces acting on its membrane and they are, respectively, area force, volume force, bond force and bending force. These forces are classified as per the follows.

$$F_{link} = -\frac{k_l dL}{p}\left[1+\frac{1}{\tau_l^2 - dL^2}\right],\ dL = \frac{L_i - L_o}{L_o} \tag{1}$$

$$F_{bend} = -\frac{k_b d\theta}{L_o}\left[1+\frac{1}{\tau_b^2 - d\theta^2}\right], d\theta = \theta_i - \theta_o \tag{2}$$

$$F_{area} = -\frac{K_a dA}{L_o}\left[1+\frac{1}{\tau_a^2 - dA^2}\right],\ dA = \frac{A_i - A_o}{A_o} \tag{3}$$

$$F_{volume} = -\frac{K_v dV}{L_o}\left[\frac{1}{\tau_v^2 - dV^2}\right],\ dV = \frac{V - V_o}{V_o} \tag{4}$$

These forces are linearly dependent on different modes of RBC deformation through independent constants (κl, κb, κa κv) and the cytoskeleton effect (τ_l, τ_b, τ_a, τ_v). Here L, Θ, A, V denote the edge length of a mesh element, angle between two adjacent mesh elements, area of triangular patch and the volume of the cell, respectively. 0 is the equilibrium value for each variable and is determined immediately after the cell's equilibrium state has been produced without any external forces [1, 9].

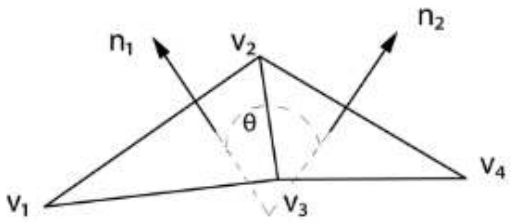

Figure 1:Two adjacent triangles with notations [1]

The implementation of the above-mentioned force terms [Eq (1), (2), (3) and (4)] can be explained as follows. Consider two adjacent triangles of the RBC mesh (Figure 1). For each edge $\vec{e_i}, i \in [1..Ne]$ the link force is added to the end node of that edge. The link force represents the response to the stretching and compression of the cytoskeleton structure. The link force of the edge between the nodes $\vec{v}_1$ and $\vec{v}_2$ can be shown as follows.

$$\vec{F}_{link_{v1}} = F_{link} \times \frac{\vec{v}_2 - \vec{v}_1}{||\vec{v}_2 - \vec{v}_1||} = -\vec{F}_{link_{v2}} \tag{5}$$

The bending force acts between two adjacent mesh triangles and represents the bending response of both the membrane and the cytoskeleton for bending. The bending force is applied to each edge $\vec{e_i}, i \in [1..Ne]$ on the four nodes of the two triangles.

$$\vec{F}_{bend_{v_k}} = -F_{bend} \times \vec{n}_k, k \in [1,2] \tag{6}$$

$$\vec{F}_{bend_{v_l}} = F_{bend} \times \frac{\vec{n}_1 + \vec{n}_2}{2}, l \in [3,4] \tag{7}$$

The local area force acts on each surface triangle $\overrightarrow{f_j}, j \in [1..Nt]$ and reflects the reaction to stretching and compression from the combination of the bilayer and the cytoskeleton. For the surface triangle with the normal vector $\vec{n}_1$ and centroid $\vec{C}$;

$$\vec{F}_{area_{v_m}} = F_{area} \times (\vec{C} - \vec{v}_m), m \in [1,2,3] \quad (8)$$

The volume fore is here only the global term and is used to maintain the cell's quasi-incompressibility. The force is applied at each surface triangle node and points the normal surface outward. S_j is the area of j[th] triangle and S_{avg} is the average area of the triangle.

$$\vec{F}_{volume_j} = F_{volume} \times \frac{S_j}{S_{avg}} \times \vec{n}_j \quad (9)$$

The values of coefficients (κl, κb, κa κv) are dependent on the computational grid and should be selected to reproduce the real mechanical properties of RBCs (Young's modulus, bending modulus, shear modulus and Poisson 's ratio). Apart from these constants, when measuring these forces, the cytoskeleton effect is also considered. The cytoskeleton effect should be chosen in such a way as to avoid unphysical changes in the RBC model. For more details on these forces, see Zavodszky et al [1]

The required minimum particle resolution of the RBC membrane was determined by Geekiyanage et al [10] to be in the triangular mesh membrane as 2,562 vertices, 5,120 edges and 7,680 faces. This mesh resolution was selected as the most suitable triangulation mesh for the current simulation, since it fulfils the requirements of minimum triangulation quality and membrane resolution as mentioned in [10, 11]. The mesh resolution of Hemocell was thus increased up to 2,562 vertices, 5,120 edges and 7,680 faces (See Figure 2). κl, κb, and κa are the free parameters of this model and these are chosen to satisfy the results of the optical-tweezer stretching experiments (by Suresh at el [12]) and the single hexagonal patch simulation in [1] as shown below.

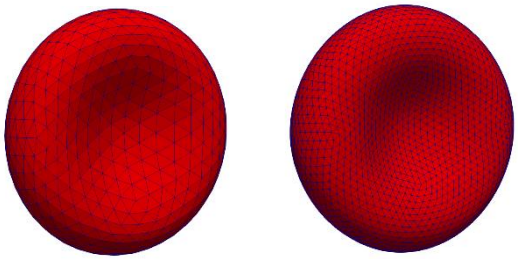

Figure 2: RBC with 642 nodes (left) and 2562 nodes (right)

Validation

A single hexagonal patch simulation (as in [1]) was employed to find the κl and κa, parameters first. As shown in Figure 3, uniaxial stretching, shearing and area expansion tests were employed in the hexagonal patch. The outcomes of the simulation results yield the κl value to be 7 kBT and κa to be 5 kBT giving the surface Young modulus of Es = 29.85 μN/m. Previous experimental values yield Es to be 25 − 50 μN/m [13], and our Es values is within this range. The shear deformation μ is equivalent to 10.15 μN / m, which is similar to the upper region of 6 − 10 μN / m reported ranges in [14, 15]. Next, the K = 28.2 μN / m compression module is close to the 18 − 20 μN / m measured range [15]. Assuming homogeneous isotropic linear behaviour (that only holds for small deformations) measured Poisson's ratio is 0.33 corresponding to the expected value of 1/3 [1].

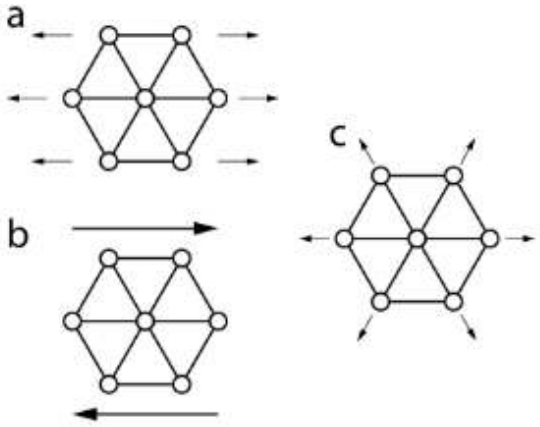

Figure 3:Mechanical tests on the patch, (a)uniaxial stretching (b)shearing (c)area expansion [1]

Then to find the κb value two adjacent triangles of the mesh were selected as a patch. Then this membrane section can be assumed as a thin plate on which the Kirchhoff-Love bending theory [16, 17] can be applied to. According to the theory, the bending moment around the x axis can be obtained as, $M_x = D\frac{\partial\theta}{\partial x}$, where D is the bending stiffness and $\frac{\partial\theta}{\partial x} = k$, k being the local curvature at the adjacent length. From this simulation kb was chosen as 50 k_BT and is equal to the bending modulus calculated by Evans [18].

Then these selected (k) parameters are employed in the model and the optical tweezer stretching experiments of Mills et al.[19] were reproduced numerically to test the parameters. The procedure using optical tweezers is conducted in such a way that tiny silica beads are connected to the opposite sides of the cell and one is fixed to the wall of the experimental container while the other is pulled away by force. The forces cause the RBC to stretch along the longitudinal axis and contract along the transverse axes. Similar to this experiment, we applied a force on the RBC's opposing ends to the five per cent of the membrane region. Those areas reflect the silica beads' attachment surfaces [1, 19].

Table 1: RBC parameters used in the RBC model

Parameter	Current Simulation (n=2562)
Equilibrium length (L0)	0.25 μm
k_BT	4.100531391×10-21 m^2kg/s^2
κl	7.00 k_BT
κb	50.00 k_BT
κa	5.00 k_BT
κv	20.0 k_BT
τ_l	3.00
τ_b	$\pi/6$
τ_a	0.3
τ_v	0.01

Results of the experiment is shown in Figure 4. The upper curve shows an axial diameter expansion due to stretching force, while the lower one reflects the transverse contraction of the cell.

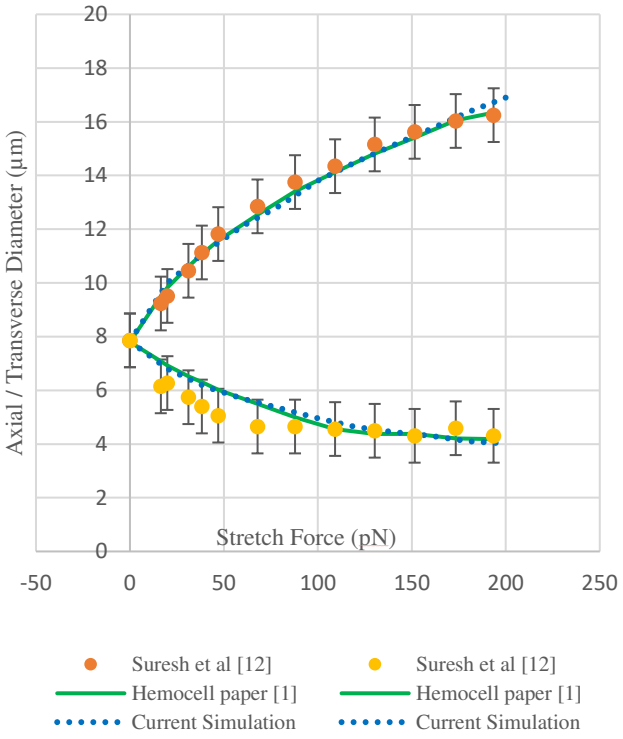

Figure 4: The outcomes of the RBC stretching simulations. The upper curve represents expansion of the axial diameter, while the lower curve reflects the cell's transverse contraction.

Flow through nonuniform capillary

Previous numerical simulations using smoothed particle hydrodynamics (SPH) method [20] have modelled the flow of discocytes through a nonuniform capillary. The same numerical simulation is reproduced using the LB-IB method for validation. Therefore, the geometrical parameters of the capillary, was selected same as the reference [20] (see Figure 5). The total length of the stenosed capillary in x-direction is 31.2 µm, diameter of the inlet and outlet are 10.2 µm and the minimum height at the stenotic area is about 6.75 µm.

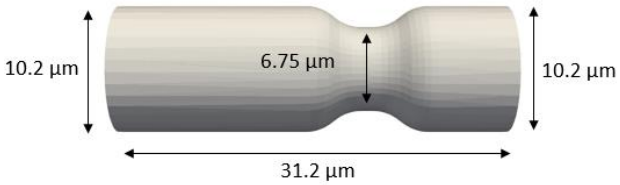

Figure 5: Solid model of the capillary

Reynolds number was selected as in reference [20] to 0.06. Then the initial velocity 0.04 ms^{-1} was given to the fluid at the inlet. The RBC continues going with plasma flow because of the applied velocity (0.04 mm/s) in the inlet. When an RBC flows through the capillary, it deforms, and the initial RBC biconcave shape is modified to the parachute shape.

The deformation of RBC can be measured with the time using Deformation Index and it can be defined as in Eq. (9)

$$DI = \frac{RBC\ length\ in\ X\ direction}{RBC\ length\ in\ Z\ or\ Y\ direction} \qquad (10)$$

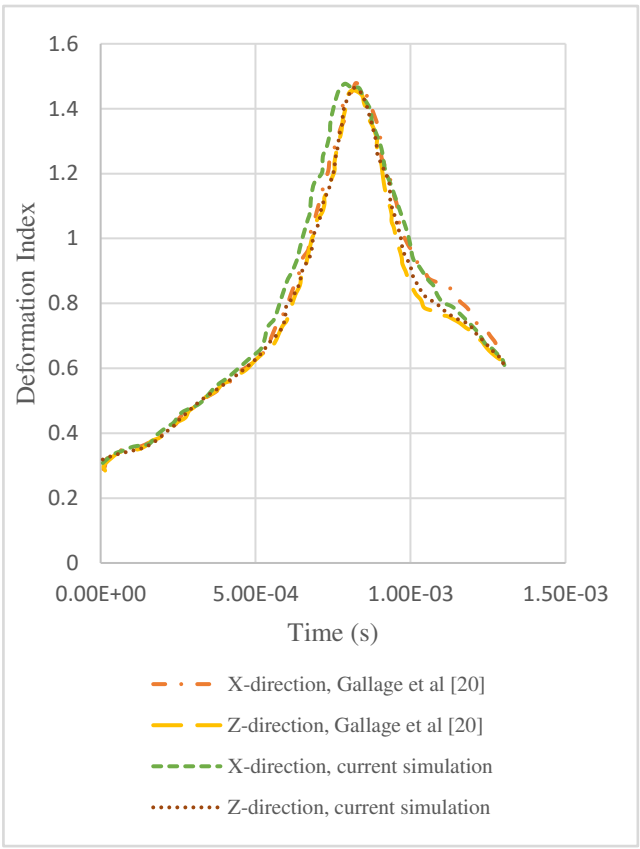

Figure 6: The variation of DI with time

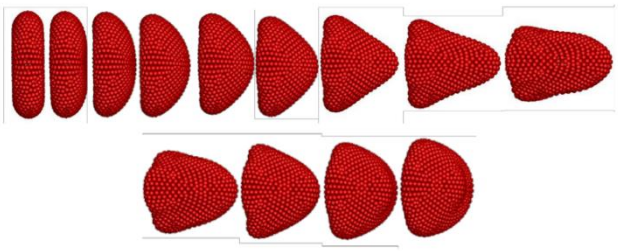

Figure 7: The flow of Discocyte through the non-uniform capillary by Gallage et al [20]

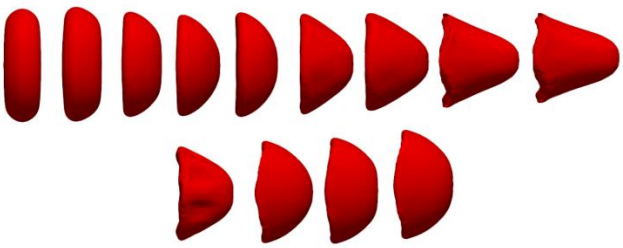

Figure 8: The flow of Discocyte through the non-uniform capillary (current simulation)

The RBC initially flows through a segment where the capillary diameter is uniform, and the RBC's DI increases slowly over that period (see Figure 6) until it reaches the stenosed area. When the RBC reaches the capillary cross-sectional area is suddenly reduced, the RBC's DI rises drastically with the time and the DI variation shows similar pattern with the RBC 's position. This, however, can be seen from Figure 6. Once the RBC squeezes through the stenosed region, the DI reaches a peak value around 1.45. The major difference in the shape of the deformed RBC, can be seen as it passes through the capillary's narrowest region. Then,

with time, the RBC's DI decreases when it leaves the capillary's stenosed region and the RBC begins to regain its normal parachute form (see Figures 7 &8). If the RBC leaves the narrowed region entirely, the RBC's DI gets approximately the same value as the inlet values. Thus, the RBC's deformation index is highly dependent on the capillary cross section through which RBC travels.

Current simulation is well agree with the [20]. The simulation time for SPH method had taken 574.8 hours (for the whole simulation with 6 CPUs of parallel processing) [20] while the LB-IB approach took only 30 minutes (with 4 CPUs of parallel processing). The fluid (plasma) is discretised into a finite number of particles in [20] and these moving particles are individually tracked. They have their own position, velocity, and time. But in LB method, particles (45900 particles are used in current simulation) are not individually tracked, but their statistics is considered. Statistic is reconstructed from the particles whose position and velocity lie on a lattice grid. This is the reason for fastness of LB method over SPH method.

Conclusion

Using the LB-IB method, the RBCs deformation behaviour was studied via a non-uniform capillary. This work demonstrates that LB-IB method is both efficient and accurate tool for analysing complex fluid systems. We observed that the capillary 's geometric shape, through which RBCs move, effects the RBC's deformation index significantly. If the capillary comprises a narrowed section, the RBCs are subjected to greater deformation. However, the deformation property of the RBCs should be examined when interacting with other RBCs in future works to get more realistic results.

Acknowledgments

The authors would like to acknowledge the support provided by Dr. NM Geekiyanage, QUT's High-Performance Computer Resources (HPC). Special thanks are extended to Dr. Gabor Zvadaszky and Mr. Victor Azizi for allowing HEMOCELL as open software and for their guidance throughout the project.

References

[1] Zavodszky G., van Rooij B., Azizi V., and Hoekstra A., "Cellular Level In-silico Modeling of Blood Rheology with An Improved Material Model for Red Blood Cells," *Front Physiol,* vol. 8, p. 563, 2017.

[2] Mchedlishvili G. and Maeda N., "Blood Flow Structure Related to Red Cell Flow: A Determinant of Blood Fluidity in Narrow Microvessels," *Japanese Journal of Physiology,* vol. 51, pp. 19-30, 2001.

[3] Tsubota K., Wada S., and Yamaguchi T., "Particle method for computer simulation of red blood cell motion in blood flow," *Comput Methods Programs Biomed,* vol. 83, pp. 139-46, Aug 2006.

[4] Mohandas N. and Gallagher P. G., "Red cell membrane: past, present, and future," *Blood,* vol. 112, pp. 3939-48, Nov 15 2008.

[5] Fedosov D. A., Caswell B., and Karniadakis G. E., "A multiscale red blood cell model with accurate mechanics, rheology, and dynamics," *Biophys J,* vol. 98, pp. 2215-25, May 19 2010.

[6] Pozrikidis C., "Numerical Simulation of the Flow-Induced Deformation of Red Blood Cells," *Annals of Biomedical Engineering,* vol. 31, pp. 1194–1205, 2003.

[7] Tomaiuolo G., "Biomechanical properties of red blood cells in health and disease towards microfluidics," *Biomicrofluidics,* vol. 8, p. 051501, Sep 2014.

[8] Z´avodszky G. a., Rooij B. v., Azizi V., Alowayyed S., and Hoekstra A., "Hemocell: a high-performance microscopic cellular library," presented at the International Conference on Computational Science, ICCS 2017, Zurich, Switzerland, 2017.

[9] Nikfa M., Razizadeh M., Zhang J., Paul R., Wu Z. J., and Liu Y., "Prediction of Mechanical Hemolysis in Medical Devices via a Lagrangian Strain-Based Multiscale Model," *Artif Organs,* Feb 3 2020.

[10] Geekiyanage N. M., "Numerical Investigation of Recoverability of Morphological And Deformabality Changes of Stored Red Blood Cells," Doctor of Philosophy, School of Chemistry, Physics and Mechanical Engineering, Science and Engineering Faculty, Queensland University of Technology, 2020.

[11] Geekiyanage N. M., Balanant M. A., Sauret E., Saha S., Flower R., Lim C. T.*, et al.*, "A coarse-grained red blood cell membrane model to study stomatocyte-discocyte-echinocyte morphologies," *PLoS One,* vol. 14, p. e0215447, 2019.

[12] Dao M., Lim C. T., and Suresh S., "Mechanics of the human red blood cell deformed by optical tweezers," *Journal of the Mechanics and Physics of Solids,* vol. 51, pp. 2259-2280, 2003.

[13] Yoon Y. Z., Hong H., Brown A., Kim D. C., Kang D. J., Lew V. L.*, et al.*, "Flickering analysis of erythrocyte mechanical properties: dependence on oxygenation level, cell shape, and hydration level," *Biophys J,* vol. 97, pp. 1606-15, Sep 16 2009.

[14] Mohandas N. and Evans E., "Mechanical properties of the Red Cell Membrane in relation to molecular Structure and genetic defects," *Annu. Rev. Biophys. Biomol. Struet.,* vol. 23, pp. 787-818, 1994.

[15] Park Y., Best C. A., Kuriabova T., Henle M. L., Feld M. S., Levine A. J.*, et al.*, "Measurement of the nonlinear elasticity of red blood cell membranes," *Phys Rev E Stat Nonlin Soft Matter Phys,* vol. 83, p. 051925, May 2011.

[16] Volino P., Courchesne M., and Thalmann N. M., "Versatile and Efficient Techniques for Simulating Cloth and Other Deformable Objects," 1995.

[17] B. Thomaszewski M. W., "Bending Models for Thin Flexible Objects," *Short Communications proceedings,* vol. 09, 2006.

[18] Evans E. A., "Bending Elastic Modulus of Red Blood Cell Membrane derived from buckling instability in Micropipet Aspiration Tests," *Biophysics Journal,* vol. 43, pp. 27-30, 1983.

[19] Mills J. P., L.Qie, Dao M., T.Lim C., and Suresh S., "Nonlinear Elastic and Viscoelastic Deformation of the Human Red Blood Cell with Optical Tweezers," *Mech. Chem. Biosyst.,* vol. 01, pp. 169-180, 2004.

[20] Gallage H. N. P., Saha S. C., and Gu Y., "Deformation of a three-dimensional red blood cell in a stenosed micro-capillary," presented at the 8th Australasian Congress on Applied Mechanics, ACAM 8, Melbourne, Australia, 2014.